Coatability of Cellulose Nanofibril Suspensions: Role of Rheology and Water Retention

Vinay Kumar,[a,*] Vegar Ottesen,[b] Kristin Syverud,[b,c] Øyvind Weiby Gregersen,[b] and Martti Toivakka [a]

Cellulose nanofibril (CNF) suspensions are not easily coatable because of their excessively high viscosity and yield stress, even at low solids concentrations. In addition, CNF suspensions vary widely in their properties depending on the production process used, which can affect their processability. This work reports roll-to-roll coating of three different types of CNF suspensions with a slot-die, and the influence of rheology and water retention on coatability is addressed. The impact of CMC addition on the high and low shear rate rheology, water retention, coatability, and final coating quality of these suspensions is reported. All three CNF suspensions were coated successfully using the slot-die coating process. CMC addition further improved the coatability by positively influencing both the low and high shear rate viscosity and water retention of the CNF suspensions. All CNF coatings significantly improved the air, heptane vapor, grease and oil barrier, while reducing the water vapor transmission rate to some extent.

Keywords: Roll-to-roll coating; Slot-die; Cellulose nanofibrils; Water retention; Low and high shear rate rheology

*Contact information: a: Laboratory of paper Coating and Converting, Center for Functional Materials, Åbo Akademi University, Turku, Finland; b: Department of Chemical Engineering (IKP), Norwegian University of Science and Technology (NTNU), Trondheim, Norway; c: Paper and Fibre Research Institute (PFI), NO-7491 Trondheim, Norway; *Corresponding author: vkumar@abo.fi*

INTRODUCTION

Environmental benefits, such as sustainability, biodegradability, renewability, and biocompatibility, have led to a significant interest in bio-based raw materials such as cellulose nanomaterials. These, in one form or another, have been tested in a wide spectrum of applications in the past decade. Numerous literature reviews, doctoral theses, and book chapters have recently covered applications spanning food packaging (Johansson *et al.* 2012; Paunonen 2013; Khan *et al.* 2014; Li *et al.* 2015; Azeredo *et al.* 2016; Hubbe *et al.* 2017), composites (Siqueira *et al.* 2010; Spence *et al.* 2011; Khan *et al.* 2014; Lee *et al.* 2014; Khalil *et al.* 2016), rheology modification and colloid science (Dimic-Misic 2014; Salas *et al.* 2014), and biomedical uses (Lin and Dufresne 2014; Plackett *et al.* 2014; Hua 2015; Jorfi and Foster 2015; Liu *et al.* 2016) to printed and flexible electronics (Zheng *et al.* 2013; Kim *et al.* 2015; Hoeng *et al.* 2016). Based on the production method used, these plant-derived cellulose nanomaterials have been classified into two main categories: cellulose nanocrystals (CNC) and cellulose nanofibrils (CNF). CNCs are mostly prepared by acid hydrolysis of cellulose fibers (Nickerson and Habrle 1947; Rånby 1949; Marchessault *et al.* 1959), and the progress in the production and characterization of CNCs has been reviewed recently (Habibi *et al.* 2010; Ramires and Dufresne 2011; Mariano *et al.* 2014; George and Sabapathi 2015). CNFs, on the other hand, are manufactured by

mechanical fibrillation of cellulose fibers using high shear forces (Turbak *et al.* 1983). Enzymatic (Pääkkö *et al.* 2007) and/or chemical pretreatments, such as TEMPO-mediated oxidation (Saito and Isogai 2004; Saito *et al.* 2006) or carboxymethylation (Wågberg *et al.* 2008), have also been applied to reduce the energy consumption and simultaneously improve the degree of fibrillation during mechanical processing. A vast amount of literature reviews addressing various aspects of CNFs (Eichhorn *et al.* 2010; Isogai *et al.* 2011; Klemm *et al.* 2011; Moon *et al.* 2011; Lavoine *et al.* 2012; Isogai 2013; Brodin *et al.* 2014; Osong *et al.* 2016; Nechyporchuk *et al.* 2016a) have been published in a short span of time, demonstrating the enormous attention CNFs have gathered from the scientific community.

Rheology and water retention of traditional pigment coating suspensions are some of the key parameters controlling their coatability. It is even more important to characterize these properties for CNF suspensions due to their complex flow behavior and high water content. Rheology of CNF suspensions has been studied in detail by many research groups (Pääkkö *et al.* 2007; Lasseuguette *et al.* 2008; Agoda-Tandjawa *et al.* 2010; Iotti *et al.* 2011; Mohtaschemi *et al.* 2014; Nechyporchuk *et al.* 2014; Naderi and Lindström 2016; Nazari *et al.* 2016; Schenker *et al.* 2016) over the past decade, and has been critically evaluated in a recent book chapter by Naderi and Lindström (Naderi and Lindström 2015) and a review by Nechyporchuk *et al.* (2016b). Most of these studies report rheological behavior of CNF suspensions in boundary-driven flow. Pressure-driven flow behavior, which is also important for processing purposes, has not received much attention excepting some recent studies (Moberg *et al.* 2014; Haavisto *et al.* 2015; Kumar *et al.* 2016b). There have been many studies on water retention of CNF suspensions (Turbak *et al.* 1983; Saito *et al.* 2007; Cheng *et al.* 2010; Lahtinen *et al.* 2014), but there is a lack of research work on the role of water retention of CNF suspension on its processability into coatings. Dimic-Misic (2014) and Rantanen *et al*. (2015) reported improvement in water retention of pigment suspensions with CNF addition. Kumar *et al*. (22016a) and Mousavi *et al*. (2017) recently reported the water retention of mechanically produced pure CNF suspensions and its impact on the coating quality obtained. However, there is still a need to understand the difference between water retaining abilities of various CNF types and the role it plays in their coatability.

Coating of CNF suspensions has been of high interest to the scientific community in the past decade. Syverud and Stenius (2009) and Aulin *et al.* (2010) were among the first to report an improvement in air resistance of paper with microfibrillated cellulose (MFC) coating. Kinnunen-Raudaskoski *et al*. (2014) and Beneventi *et al*. (2014) used foam coating and spray coating techniques, respectively to apply nanocellulose on paper and reported a reduction in air permeability. Lavoine *et al*. (2014a) reported improvement in strength properties of cardboard with MFC coating applied using bar coating process. The same group (Lavoine *et al.* 2014b) also reported comparison between two different MFC coating application techniques: bar coating and size press. They observed considerable improvement in air barrier and bending stiffness of paper coated with MFC using bar coating. Afra *et al.* (2016) showed that CNF coating improves surface smoothness, surface strength, tensile strength, stiffness and air resistance of paper. At the same coat weights, a double coating layer applied at low solids (1.5 wt%) concentration performed better than a single coating layer applied at high solids (3 wt%) concentration. Herrera *et al.* (2016) reported dip and spin coating techniques of nanocellulose on two different porous cellulose substrates. They found the dip coating technique to be more suitable for the substrate with large pore size because the thick coating applied with this technique delaminated from the

substrate with small pores. On the other hand, the spin coating technique was more suitable for the substrate with small pore size due to insufficient coverage obtained with spin coating in case of the substrate with large pores. They also saw improvement in oxygen barrier with nanocellulose coating, but prolonged storage and humidity diminished the barrier performance. In a later study, the same group (Herrera *et al.* 2017) used a dip coating technique to apply nanocellulose as thick multilayers on a porous paper, and plasticization of nanocellulose coating with sorbitol or cross-linking with citric acid were found to improve the water vapor and oxygen barrier. Improvement in anti-bacterial functions of substrate with CNF coating was recently reported by Amini *et al*. (2016), where they utilized colloidal silver (Ag) nanoparticles in the coating. Water vapor transmission rate, oil resistance, and tensile strength of CNF/Ag coated papers were improved as well. Some groups have also reported printability improvements with nanocellulose coating on paper (Song *et al.* 2010), and woven and non-woven fabrics (Hamada and Mitsuhashi 2016). In addition, Hamada and Mitsuhashi observed an improvement in air resistance and heat retention properties of fabrics with CNF coating. Mousavi *et al*. (2017) recently reported drawdown rod coating of mechanically produced CNFs on paperboard to improve air, water, moisture, and grease barrier performance and found that CMC used as an additive improved coatability and final coating quality. In addition, a higher degree of fibrillation of CNF material led to more uniform coating and thus superior barrier performance. Ridgway and Gane (2012) and Kumar *et al*. (2017) reported the impact of substrate properties on coatability of mechanically produced CNF suspensions and the final coating quality obtained. Kumar *et al*. (2017) found a smooth, but porous, and highly hydrophilic substrate to be an optimal choice for nanocellulose coating application. Ridgway and Gane (2012) investigated coating uniformity and holdout of CNF on a base paper and an absorbent pre-coating layer. CNF showed excellent holdout on absorbent pre-coating layer contrary to the base paper, leading to a higher improvement in paper stiffness and surface properties when applied on the porous pre-coating layer. Recently, Hubbe *et al*. (2017) have provided a thorough review of literature on nanocellulose used in coatings.

Most reports so far have been based on small-scale batch processed coatings. Continuous coating of CNF suspensions is of interest for it to be relevant for industrial-scale production. However, there are various challenges associated with continuous coating of CNF suspensions. CNF suspensions are highly viscous and demonstrate yield stress behavior, making it difficult to pump them to the coating unit and subsequently form a thin wet film. They also contain large amounts of water, usually more than 95 wt%, which makes it challenging to dry the coating; paper-based substrates may not withstand such large amounts of water, leading to runnability problems such as web breaks. One of the recent processes reported by the authors of this work enabled roll-to-roll coating of CNF suspension by utilizing its shear thinning behavior (Kumar *et al.* 2016a; Ottesen *et al.* 2017). CNFs can differ considerably in their properties depending on the production method used (Syverud *et al.* 2011; Kumar *et al.* 2014; Naderi and Lindström 2016). It is therefore important to determine how different CNF suspensions behave when coated using the said process. In addition, there has been a lack of research work addressing the role of rheology, especially at high shear rates, and water retention on the coatability of CNF suspensions. An understanding of the rheological and water retention properties of CNF suspensions can give insight into their behavior in a coating process. The main objectives of this work are therefore as follows:

1. To determine the coatability of three different types of CNF suspensions in a roll-to-roll process and specifically understand the influence of rheology and water retention on the same;
2. To understand the impact of CMC addition on water retention and rheological properties of these suspensions, and their relation to coatability; and
3. To investigate barrier properties to gain insights into the final coating quality achieved.

The aim of this study is to enrich further the understanding of the coatability of different nanocellulose materials for various applications.

EXPERIMENTAL

Materials

Three different types of dilute cellulose nanofibril (CNF) suspensions (0.85% solids) were produced using the methods described in Table 1. A Rannie15 type 12.56× homogenizer (APV, SPX Flow Technology, Silke-borg, Denmark) was used for mechanical fibrillation of the pre-treated samples. In all cases, the first pass through the homogenizer was at 600 bar pressure drop, while 1 kbar pressure drop was used for all subsequent passes. Each of the three produced CNF types were divided into two separate batches after fibrillation. One batch was kept without further modification, while the other received an addition of 5 wt% (on total solids) of carboxymethyl cellulose (CMC) FINNIFIX® 4000G (CP Kelco, Finland).

Table 1. CNF Types and Their Production Processes

CNF type	Raw material	Pre-treatment	No. of passes through the homogenizer
CNF-M	Bleached softwood Kraft pulp	Beating in Claflin mill (1000 kWh/ton for 1 h)	5
CNF-T	Bleached sulfite pulp	TEMPO-mediated oxidation (2.35 mmol ClO- per gram cellulose) according to (Saito *et al.* 2006)	2
CNF-C	Bleached sulfite pulp	Low substituted carboxymethylation (10 g monochloroacetic acid in 0.5 L isopropanol) according to (Wågberg *et al.* 2008)	3

The substrate used for coating purposes was a recycled fiber linerboard (Dong Il Paper, South Korea) with grammage and thickness of 178 ± 4 g/m^2 and 190 ± 5 μm, respectively. The PPS surface roughness of the linerboard is 7.39 ± 0.51 μm, and it is highly water absorbent, with a Cobb-60 value of approximately 250 g/m^2. The water contact angle for the linerboard is also very low, as it drops below 20° within 10 s.

Characterization of CNFs

Transmission electron microscopy (TEM) was used to determine the morphology of CNFs. For TEM sample preparation, a 0.05 wt% CNF suspension was drop casted on formvar/carbon-coated 400-mesh copper grids and negatively stained with 1% (w/v) uranyl

acetate in water for 60 s. TEM images were captured with a JEM-1400 Plus TEM (JEOL; Tokyo, Japan) using an acceleration voltage of 80 kV. The charge content of the CNFs was determined by conductometric titration, as described by Saito and Isogai (2004).

Characterization of CNF Suspensions

Water retention

The static gravimetric dewatering of CNF suspensions was measured using the Åbo Akademi Gravimetric Water Retention device (ÅA-GWR) (Sandas *et al.* 1989). For measurement, 10 mL of suspension was inserted into the cylindrical vessel placed above a 5-µm polycarbonate membrane (GE Water & Process Technologies, USA) backed by eight absorbent blotter papers. These suspensions had large amounts of water (> 99 wt%); therefore, eight instead of the usual two blotter papers were used in each measurement to avoid saturation. The pressure used for the measurement was 50 kPa for a 90-s time duration. The average of three determinations is reported. The GWR value represents the amount of water released by the suspension per unit area, and a higher value suggests lower water retaining capability.

Pressure filtration measurements were performed using the setup shown in Fig.a. For measurements, 20 mL of suspension was inserted into the cylindrical filtration chamber and subjected to a pressure of 10 bar. A 5-µm polycarbonate membrane (GE Water & Process Technologies, USA) was kept over a sturdy wire mesh over which a filter cake was formed as water was released under pressure. The amount of filtrate coming out was constantly measured over time.

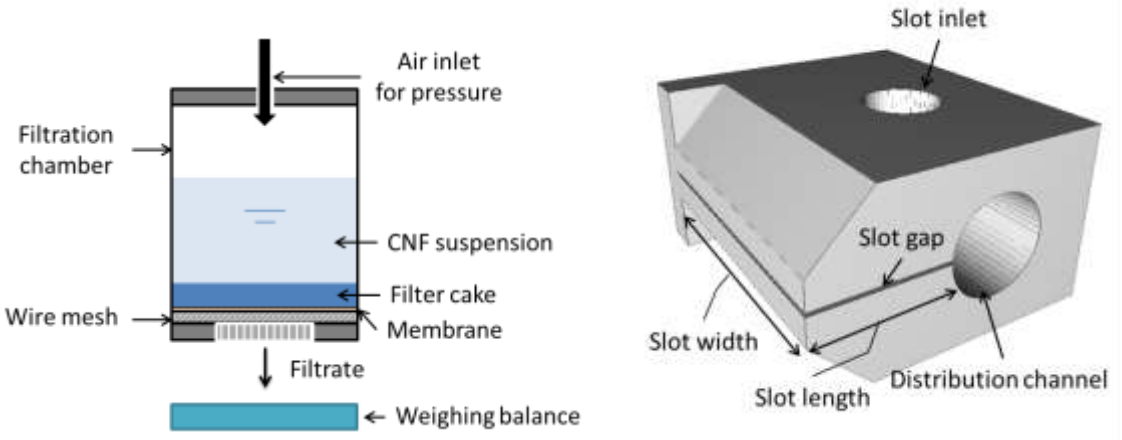

Fig. 1. Schematic of (a) pressure filtration setup and (b) the slot-die

Rheology

Steady-state viscosity measurements with parallel plate geometry were carried out using a Paar Physica Modular Compact Rheometer (MCR) 300 (Anton Paar, Austria) (plate diameter: 50 mm, gap: 1 mm). The measurements were performed in a shear rate range of 0.01 to 1000 s^{-1} without any pre-shearing protocol. However, the suspension was mixed well before carrying out the rheological measurements.

Pressure-driven flow was characterized using slot-die geometry, shown in Fig.b, as described previously (Kumar *et al.* 2016b). The slot-die consists of a distribution channel with a radius of 16 mm, a slot of length 34 mm, and a width of 74 mm. The slot gap is 1000 µm. The CNF suspension is fed into the slot inlet from an air-pressurized suspension container. The flow rate is measured gravimetrically by collecting the outflow during a

known time interval after a steady state has been achieved. Kinetic energy corrections were applied to the data as described in earlier studies (Kumar *et al.* 2016b).

Coating Process

All CNF suspensions, with and without added CMC, were coated onto the linerboard using a modified Rotary Koater (RK PrintCoat Instruments Ltd., United Kingdom). The coating process has been reported in detail previously (Kumar *et al.* 2016a). Briefly, the custom-built slot-die (Fig. 1b) was used as a coating applicator. The slot-die is fitted onto the top of a movable rail at three o'clock position to a backing roll. The distance between the slot lips and the substrate can be controlled precisely by moving the rail in the horizontal direction, perpendicular to the backing roll. The top lip of the slot acts as a metering element, and excess coating material metered off is collected in a tray underneath the slot die. A gap of approximately 600 µm was used between the slot lips and substrate during coating application, which resulted in an approximate dry coat weight of 5 to 6 g/m^2. The dry coat weight was calculated from the difference between grammages of the CNF coated and uncoated substrate. However, it should be noted that the dry coat weight calculation here is not very precise because of the large variations in grammage of the substrate itself. The substrate was 12 cm wide, and the width of the coated area was approximately 7 cm. The coating speed was 3 m/min. The substrate and CNF-coated samples were calendered with a laboratory soft nip calender (DT Paper Science Oy, Finland), keeping the back side towards the soft roll, using a line load of 100 kN/m and temperature of 60 °C. All samples were then conditioned (23 °C, 50% RH) for at least 24 h before further testing.

Characterization of Coated Boards

Scanning electron microscopy (SEM)

Surface SEM images of coated samples were recorded for a qualitative study of different CNF coatings. Samples were sputter coated with a 4-nm-thick PtPd alloy using a Cressington 208HR B (Cressington Scientific Instruments, UK) before imaging. Images were acquired with a Hitachi SU3500 SEM (Hitachi, Japan) using an acceleration voltage of 5 kV and a working distance of 30.5 mm.

Coating quality and barrier tests

Air permeability of the substrate and coated samples was determined using an L&W Air permeability tester SE-166 (Lorentzen & Wettre, Sweden) with a measurement range of 0.003 to 100 µm/(Pa·s). The average from five parallel measurements performed on different areas of each sample is reported.

(ASTM E96/E96M-05 2005) was used for measuring the water vapor transmission rate (WVTR). A similar procedure was used for determining the heptane vapor transmission rate (HVTR) as described earlier (Miettinen *et al.* 2015). For HVTR determination, 20 mL of heptane solvent was used in the cup instead of the $CaCl_2$ salt used for WVTR measurements. Heptane was poured onto a sponge to reach liquid/gas equilibrium as quickly as possible. The decrease in weight of the cup caused by the evaporation of heptane through the test sample was continuously tracked for 2 h. The results were then extrapolated to a time period of 24 h. The average of three parallel measurements for each sample is reported.

KIT Test, (TAPPI T 559 pm-96 1996), was used to determine the grease resistance. Another supporting test method reported by Vähä-Nissi (2016) was also used. Briefly, 200

µL of dyed oil, Oil Red O solution (Sigma Aldrich, USA), was placed underneath a 50-g weight on the coated side of the samples, and the back side was scanned at pre-selected intervals. This was also performed for 30-µm-thick free-standing CNF films for comparison with the CNF coating barrier performance.

The surface porosity, which can be used as a qualitative measure of coating coverage, was determined using print penetration tests. An IGT AIC2-5 tester (IGT Testing Systems, The Netherlands) was used according to the standard method (IGT-W24 2006). The results are obtained in the form of stain length, and a shorter stain indicates higher surface porosity or a more open pore structure at the surface.

RESULTS AND DISCUSSION

Properties of CNFs

TEM images of the various CNFs are shown in

Fig.Fig. 2a. One can observe that the morphology of CNF-M differed considerably from that of chemically pretreated CNFs. CNF-T and CNF-C display similarities in their fibril size, with mean diameters of 5.1 nm (CNF-T) and 3.0 nm (CNF-C). However, the fiber size distribution seems wider for CNF-M, which has a mean fibril diameter of 10.6 nm. Note that only individual fibrils were measured; fiber fragments, fibril bundles, and fibril clusters were not measured (Ottesen *et al.* 2017).

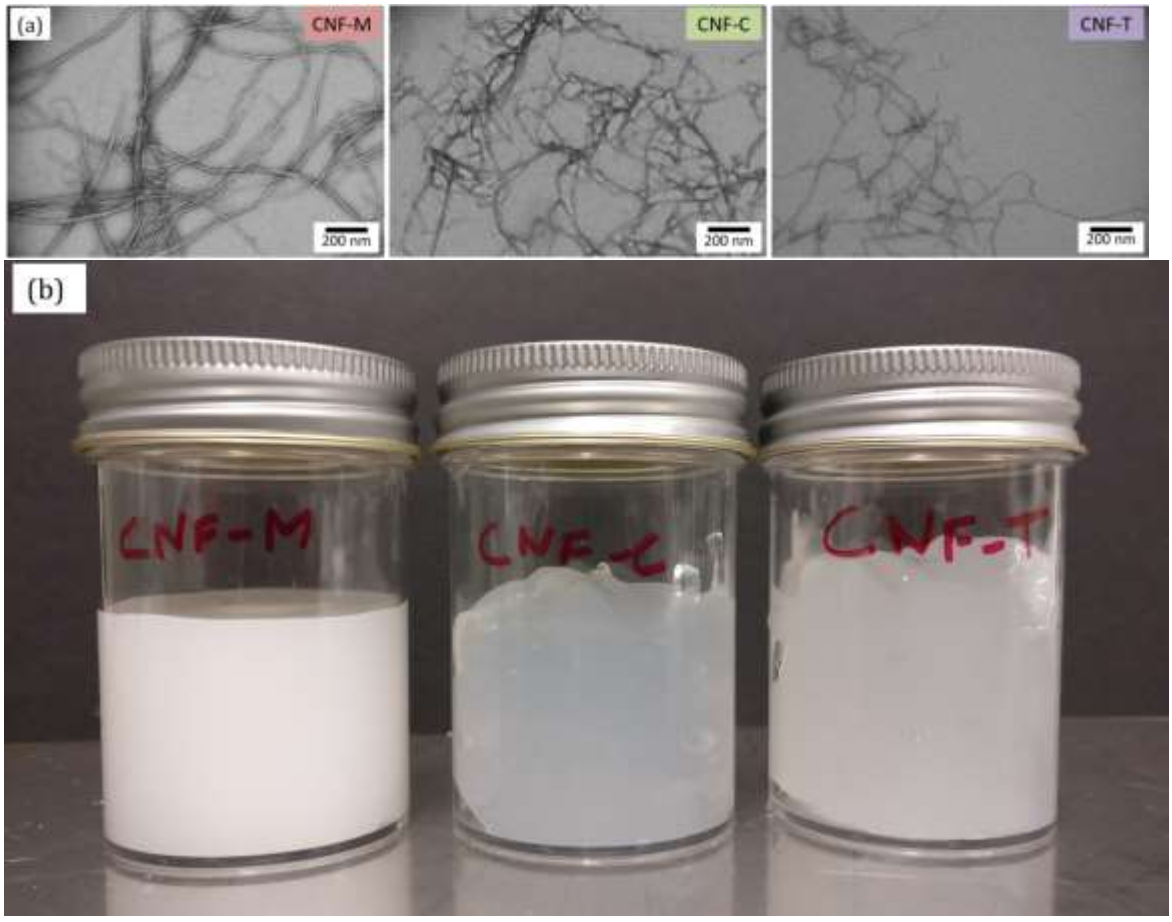

Fig. 2. TEM images of (a) the various CNFs and (b) CNF suspensions at 0.85 wt%

The charge content values of CNFs in Table 2 also show that CNF-M had a lower surface charge compared with the other two, obviously because of the chemical pretreatment used in the latter case. The charge content plays a major role in the level of fibrillation achieved during homogenization. It must be noted that a higher charge content helps reduce the number of homogenization steps required to achieve the same level of fibrillation, as is evident from CNF-T. The CNF suspensions shown in Fig. 2b indicate the level of fibrillation achieved in the three cases. CNF-M was more liquid-like and opaque because of its large fibril size and wider fibril size distribution. CNF-C and CNF-T, on the other hand, were gel-like and also more transparent compared with CNF-M. This has to do with the smaller fibril diameter and a narrow size distribution in the case of CNF-T and CNF-C. Mechanically produced CNF-M tended to flocculate, and it was less water binding and swollen than the chemically pre-treated ones, CNF-C and CNF-T. The gel-like and liquid-like behavior of CNFs is certainly expected to affect their coatability, which is discussed in subsequent sections.

Table 2. Charge Content of CNFs

Sample	Charge content (µmol/g)
CNF-M	248 ± 7
CNF-C	476 ± 64
CNF-T	910 ± 61

Water Retention and Rheology of CNF Suspensions

Water retention of coating suspensions is an important coating process parameter, as it determines the ability of coating material to resist dewatering into the substrate, which is particularly important for paper-based substrates. The CNF suspensions contained more than 99 wt% water; therefore, it is important to understand and control their water retention to coat these materials successfully. A quick release of large amounts of water from coating material into a paper-based substrate during coating can cause fiber swelling and de-bonding and may also lead to runnability problems, such as web breaks. Figure 3 shows the water retention properties of CNF suspensions. It should be noted that both dewatering evaluation methods, *i.e.*, ÅA-GWR and pressure filtration, yield static water retention values, which may differ from the actual dewatering occurring under dynamic shearing conditions during coating. However, they are reasonable indicators of how the coating material may behave during the coating process under the influence of capillary absorption into the base substrate and pressure pulses from the coating apparatus. One can observe that CNF-M clearly showed lower water retention capability compared with CNF-C and CNF-T. The high charge content and gel structure of CNF-T and CNF-C seem to have helped with improving the water retention. CNF-M also had a tendency to phase separate, thus leading to poor water retention.

The addition of CMC had a visible impact on the water retention of CNF suspensions. The water retention capability of CNF-M with CMC addition was improved, which has been observed earlier for mechanically produced CNFs (Kumar *et al.* 2016a; Mousavi *et al.* 2017). The long-chain and high-molecular weight CMC used herein may help disperse CNF-M better. This could be achieved by mechanical disentanglement and/or an overall anionic charge increase in the system. The increased dispersion could be explained also by CMC adsorption to CNF, whereby the charge repulsion between the

fibrils is increased. The tendency of CNF-M to phase separate is thus reduced, leading to higher water retention. CMC could also provide a dispersing effect in the system by decreasing the amount of free water (increasing the water phase viscosity) in the suspension, as reported in earlier studies (Vesterinen *et al.* 2010; Kumar *et al.* 2016a). Interestingly, the water retention capability of CNF-T and CNF-C was reduced upon CMC addition, as can be seen from Fig. 3a. CMC addition seems to have broken down the gel structure in both cases, which could be observed the moment CMC was added to the suspension. This effect, observed in the cases of CNF-T and CNF-C, may be explained by an increase in salt concentration of the system after CMC addition, whereby the dispersing effect may be somewhat diminished because of charge screening, as has been seen earlier when electrolytes were added to a CNF suspension (Naderi and Lindström 2014). The reduced repulsion between fibrils and thinner bound water layers leads to an increase in free water in the suspension. However, the pressure filtration results in Fig. 3b demonstrate similar behavior for all CNFs upon CMC addition. This occurs because hydrodynamic forces play a major role at higher pressures, rather than the surface chemistry of involved components. CMC, a long-chain molecule, hinders the process of dewatering at high pressures, potentially by quickly forming an entangled network. Therefore, the initial release could be quicker in the cases of CNF-T and CNF-C, but dewatering slows down as soon as the filter cake is formed. It should be noted that the solids content of CNF suspensions is maintained at 0.85%, even after CMC addition.

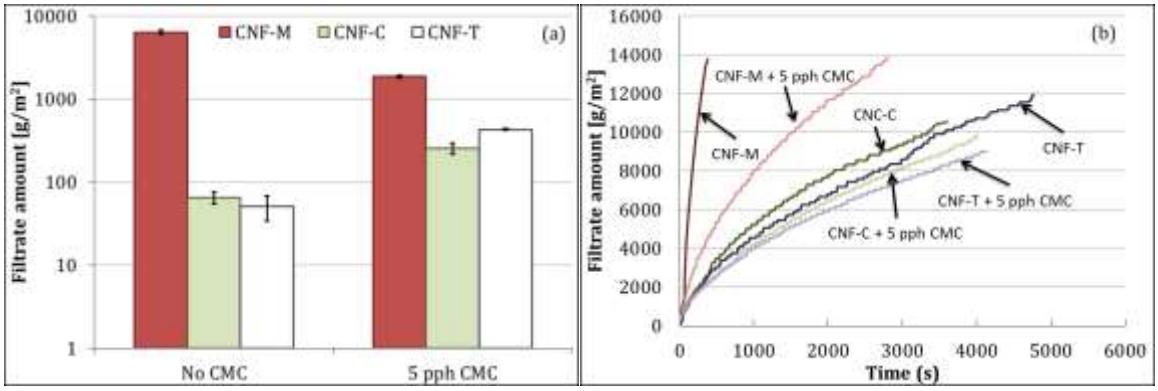

Fig. 3. Water retention of CNF suspensions with (a) ÅA-GWR and (b) pressure filtration. Error bars denote standard deviation.

Figures 4 and 5 show the well-known shear thinning rheological behavior of the CNF suspensions. The apparent suspension viscosity approached that of water at high shear rates, indicating very low flow resistance in slot flow at high flow rates. This highly shear thinning behavior could be a result of either the creation of water-rich boundary layers that promote apparent slippage, or through dynamic yielding (reduction of effective yield stress), which breaks down the suspension microstructure in the slot gap (Kumar *et al.* 2016b). CNF-M, with a power law index of 0.15, shows more shear thinning behavior compared with CNF-T and CNF-C, with power law indices of 0.27 and 0.26, respectively. CNF-M also has a lower viscosity than the other two CNFs, especially at higher shear rates. One explanation for this could be the larger fibril sizes and higher phase separating tendency of CNF-M compared with CNF-T and CNF-C, which likely leads to quicker and thicker water boundary layer formation in CNF-M, thus providing lower flow resistance. CMC addition seems to have affected the rheology differently for CNF-M compared with

CNF-T and CNF-C. CMC appears to have increased slightly the flow resistance for CNF-M, whereas it seems to have reduced the flow resistance of CNF-T and CNF-C, especially at low shear rates (up to 1000 s^{-1} in the MCR). Reduction in viscosity of CNF-T and CNF-C with CMC addition can be due to reduced flocculation of fibrils, as CMC is well known for its dispersing effect on cellulose fibers (Beghello 1998; Yan *et al.* 2006; Liimatainen *et al.* 2009) and CNF (Ahola *et al.* 2008). The dispersing effect could be higher for CNF-T and CNF-C due to their high initial charge content, which leads to further increased mutual repulsion between fibrils upon CMC addition. CMC also leads to increase in water phase viscosity, which may be contributing to the slight increase seen in case of CNF-M. However, it is difficult to state the exact reason for the opposite effect of CMC addition on viscosities of mechanically produced CNF *vs.* the chemically produced ones.

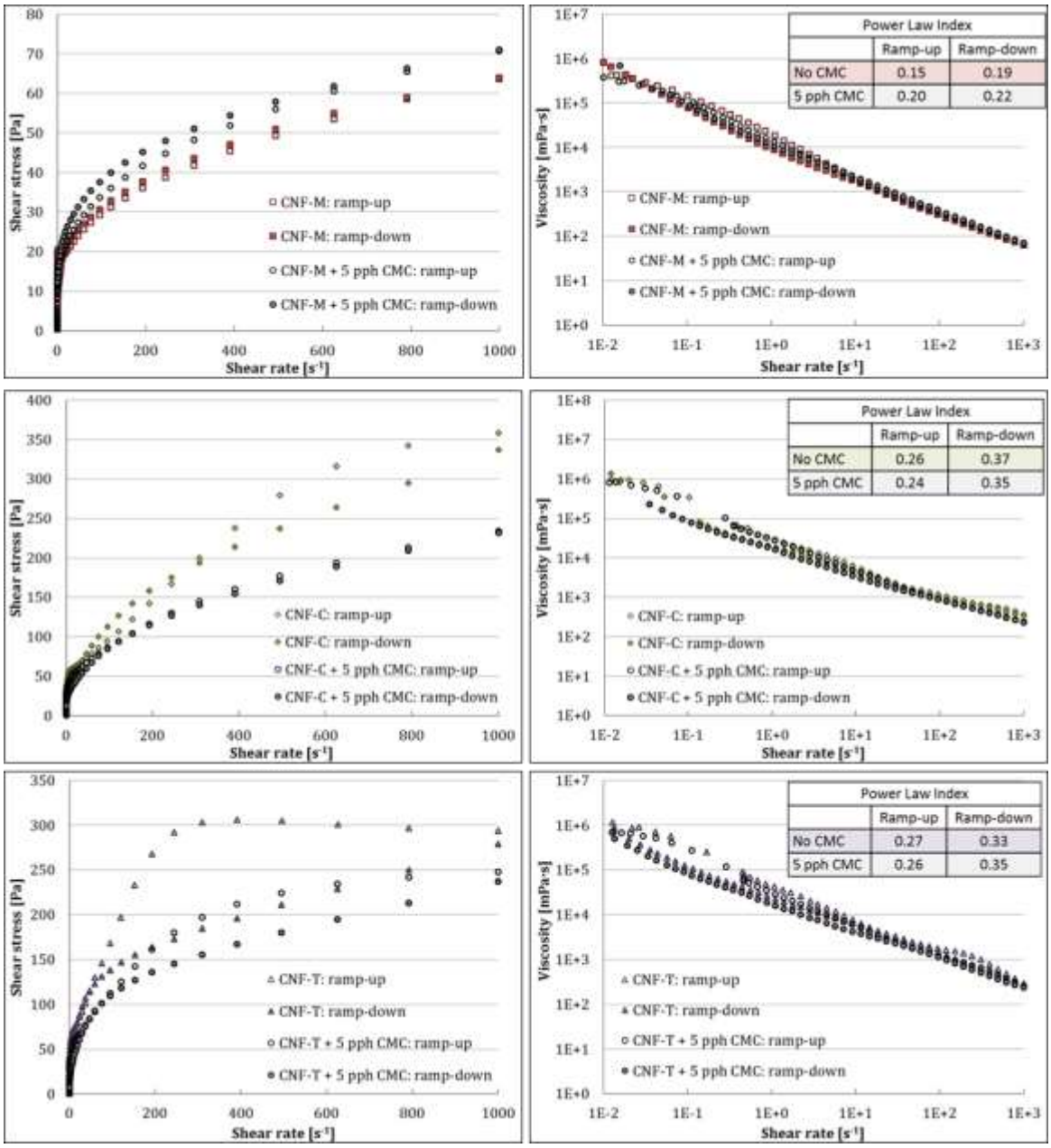

Fig. 4. Rheological properties of CNFs at low shear rates in boundary-driven flow

Figure 5 shows the high-shear rate rheological behavior of the CNF suspensions. The shear thinning behavior seems to extend to high shear rates for CNF-T and CNF-C. However, a Newtonian plateau was observed for CNF-M at shear rates beyond 10,000 s^{-1}, which could be due to turbulence at high flow rates, as the Reynolds number, calculated using water viscosity, was above 2300 when the plateau appeared. As previously (Nikbakht *et al.* 2014; Kumar *et al.* 2016b), the Reynolds number (Re) for slot has been calculated using the equation,

$$(\mathrm{Re} = \rho v H/\mu) \quad (1)$$

where ρ is density of fluid, v is flow velocity, H is slot gap, and μ is fluid viscosity (water viscosity in this case). The role of turbulence was more pronounced for CNF-M, which can be potentially attributed to its larger fibril size and higher tendency to phase-separate compared with CNF-C and CNF-T. CMC addition had a similar impact on CNF-M, CNF-T, and CNF-C rheology at high shear rates as it did at low shear rates. Figure 6 compares the results obtained from MCR to those of slot flow. The viscosity values from the two instruments seem to be in good agreement, indicating that slot geometry can be positively used for understanding the behavior of CNF suspensions at high shear rates. Also, the results from slot geometry can help determine the process parameters for coating beforehand.

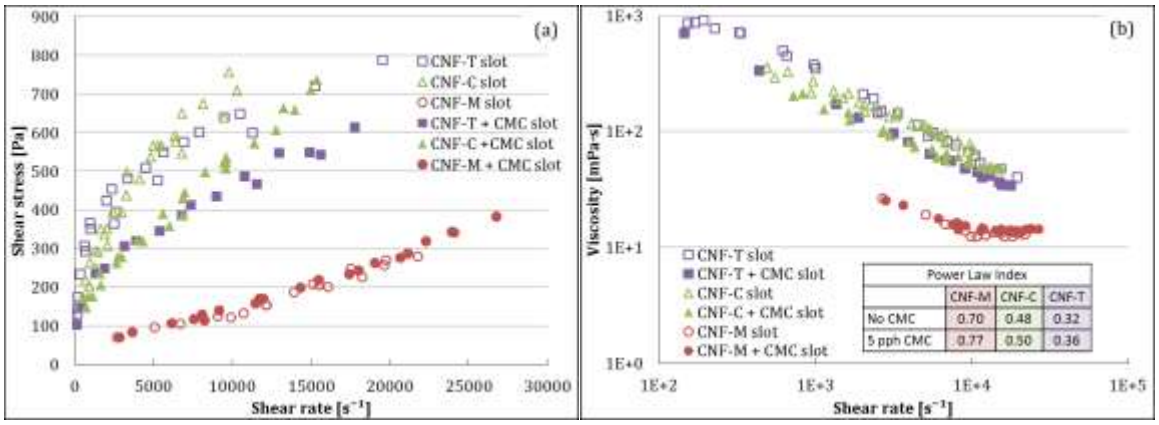

Fig. 5. Rheological properties of CNFs at high shear rates in pressure-driven flow in slot

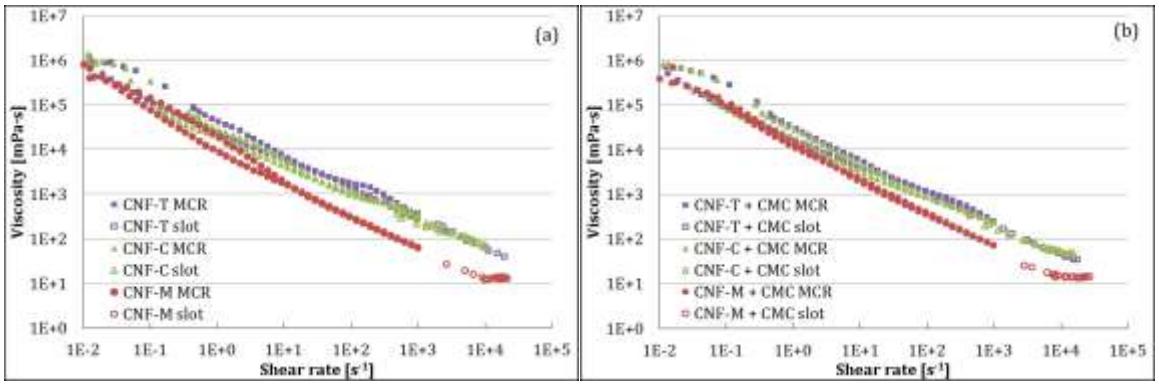

Fig. 6. Comparison of low-shear (MCR) and high-shear rheology (slot) of CNF suspensions

Yield Stress

Yield stress is another important parameter that plays a critical role in coating of these types of suspensions, as it specifies the minimum feeding pressures required to pump the suspension to the slot-die coating head. It is also highly relevant when designing slot die coating heads, as high yield stresses easily lead to undesired stagnation zones. The yield stress values for CNF suspensions calculated using the Casson model fitting are shown in Table 3. CNF-T and CNF-C demonstrated higher yield stresses compared with CNF-M, leading to higher pressures needed for feeding the slot-die. The reduction in yield stress with CMC addition indicates lower flow resistance during pumping of the suspensions to the slot die. CMC addition is thus helpful for processing purposes. The differences in yield stress between MCR and slot arise from the differing natures of the flow, *i.e.*, boundary-driven *vs.* pressure-driven, and the different geometry types.

Table 3. Calculated Yield Stress Values from Casson Fits to the Viscosity Data in Figs. 4 and 5

		Yield stress (slot data) (Pa)	Yield stress (MCR data) (Pa)
Yield stress	CNF-M	7.6	10.3
	CNF-M + CMC	5.2	8.9
	CNF-T	175.2	24.2
	CNF-T + CMC	109.6	17.9
	CNF-C	109.8	16.1
	CNF-C + CMC	74.5	16

Coatability

It is challenging to coat CNF suspensions because of their excessively high viscosity and yield stress at fairly low solids content. However, the highly shear thinning behavior of these suspensions can be utilized to coat them successfully, as demonstrated earlier by Kumar *et al*. (2016a) for mechanically produced CNF suspensions. When pushed through a narrow gap, the CNF suspensions tend to have low flow resistance, as can be seen from the high-shear rheology results in Fig. 5. This makes it possible to work with low-effective viscosity material when it has been sheared in the slot gap before coating onto the actual substrate. The slot die thus can be used both as a shearing (slot gap) and metering element (gap between the slot and substrate). The slot gap shears the material just before it enters the gap between the substrate and slot, and the excess material is metered off. The metering element works with the low-effective viscosity material, which eliminates problems such as those arising from fiber aggregation and fast structure recovery.

The CNFs used in this work seem to work well with the process described above. However, the wet film formation for CNF-T and CNF-C seems to be affected by their gel-like behavior. These materials tend to recover their structure quickly from the high-shear rate deformation applied during flow in the slot gap, which is visible from the shark skin structure observable in Fig. 7. However, CMC addition seems to break down the gel structure and delay the structure recovery, thereby leading to a uniform wet film formation during metering.

The lowered viscosity after CMC addition, as seen in the rheology results, can also play a role. CMC may also help disperse the CNFs better, thus resulting in the observed effect on wet film formation. Other researchers have also observed this dispersing effect of CMC on pulp fibers (Beghello 1998; Yan *et al.* 2006; Liimatainen *et al.* 2009) and CNFs (Ahola *et al.* 2008; Mousavi *et al.* 2017). Improvement in coating quality of mechanically produced CNFs with CMC addition has been observed in previous studies as well (Kumar *et al.* 2016a; Ottesen *et al.* 2017; Mousavi *et al.* 2017).

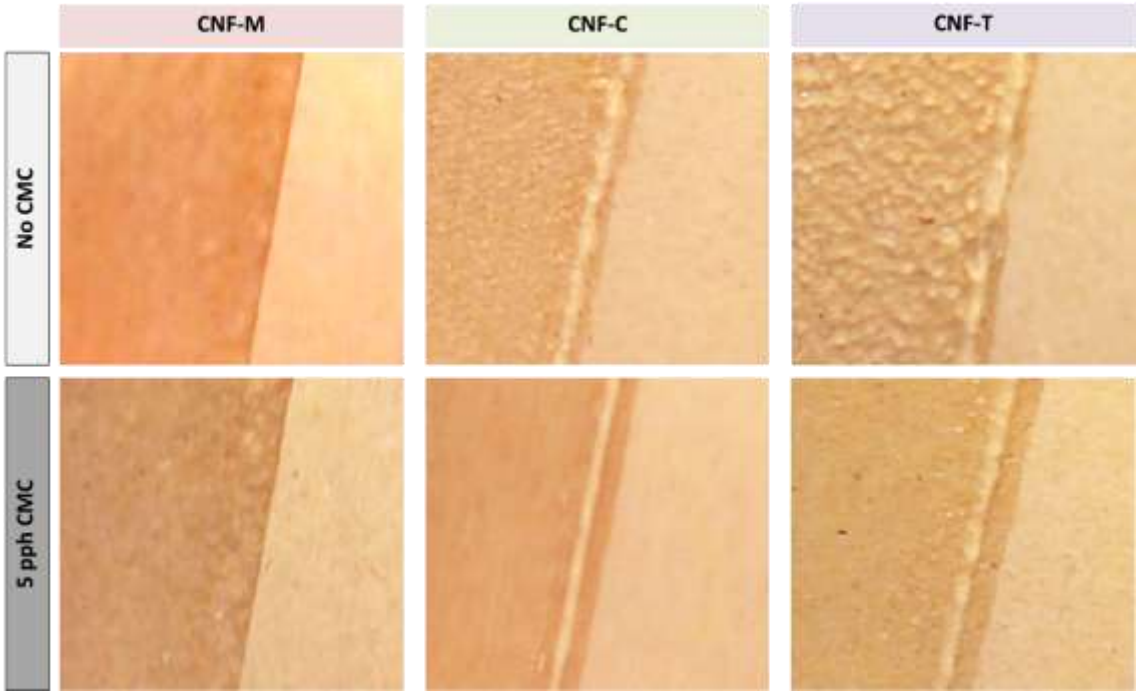

Fig. 7. CNF film formation during coating application. Shark skin effect on the wet film can be seen for CNF-C and CNF-T without CMC addition.

Properties of CNF-Coated Samples

Coated samples were characterized with respect to their coating coverage and barrier properties to understand the final coating quality achieved with different CNFs. Coating coverage was qualitatively determined from surface SEM images and print penetration tests. Figure 8 shows SEM images of the substrate and coated samples. One can clearly observe the closed structure provided by the CNF coating compared with the substrate. CNF-C and CNF-T seem to form a more closed surface structure compared with CNF-M. The coating also appears uniform, but there were some defects, such as pin holes and micro cracks alongside the fibers in the substrate (Ottesen *et al.* 2017). This is also evident from the print penetration test results in Fig. 9, which quantify the surface porosity in terms of stain length. A long stain indicates low surface porosity as the drop spreads over a large area over the closed surface. It can be established from SEM images and the print penetration test results that the reported coating process does provide a uniform coating, provided that the pinholes and defects such as cracking caused by brittleness can be eliminated.

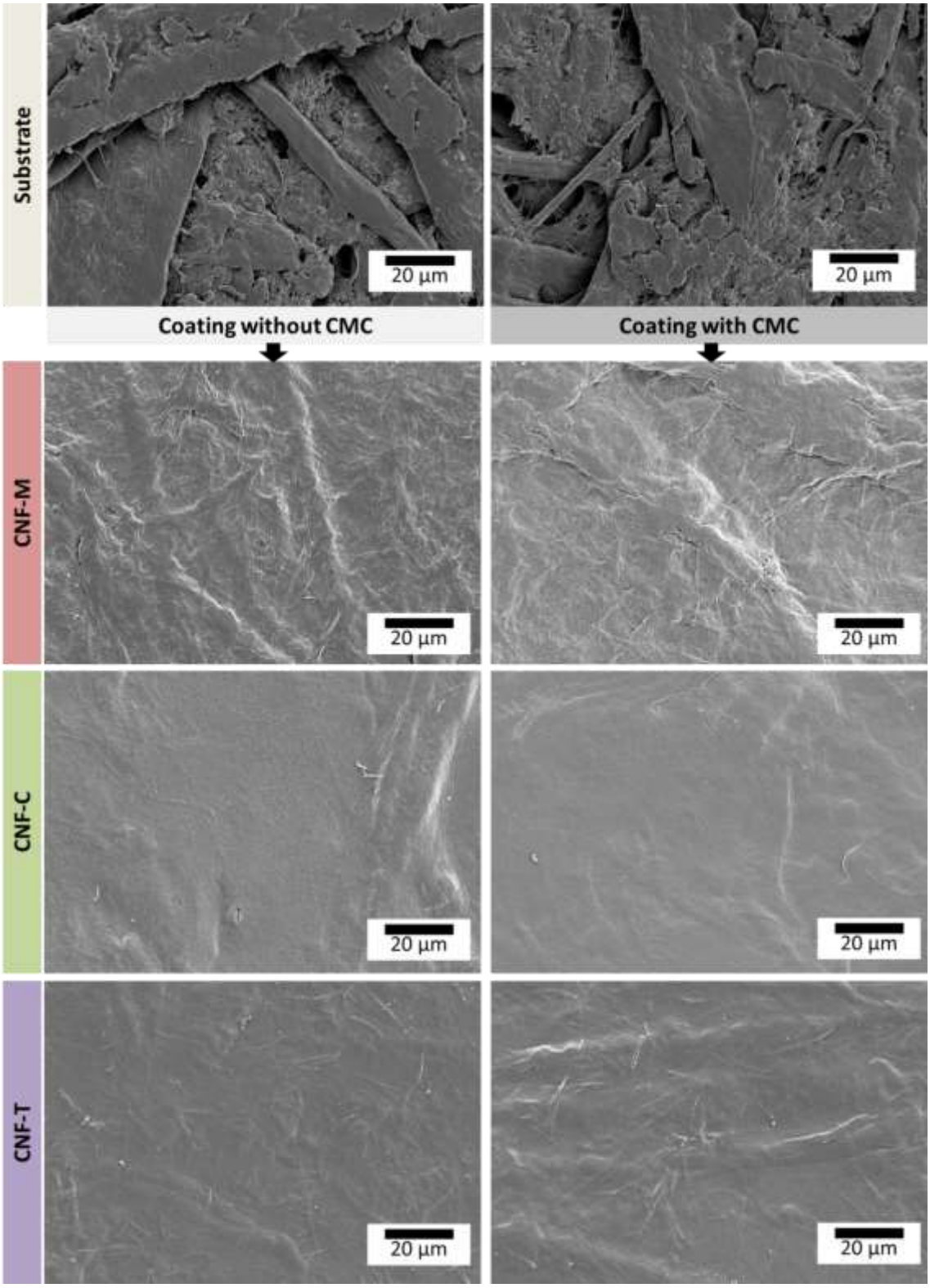

Fig. 8. Surface SEM images of CNF-coated paperboard

Air permeability values for the base substrate and CNF-coated samples are shown in Fig. 9a (Ottesen *et al.* 2017). All CNF coatings reduced the air permeability significantly, which is in agreement with previous studies (Syverud and Stenius 2009; Aulin *et al.* 2010;

Kinnunen-Raudaskoski *et al.* 2014; Beneventi *et al.* 2014; Lavoine *et al.* 2014a,b), and CNF-T and CNF-C perform better than CNF-M. However, the addition of CMC reduced the air permeability of the CNF-M coating. This is attributed to the improved water retention, potentially leading to formation of a more uniform film in the case of CNF-M. If all the water from the suspension is released instantly into the substrate, then there will be less time for uniform film formation on the surface. It is also possible that CMC simply fills in pores between the rather coarse CNF-M fibrils and thus improves the air barrier. CMC addition does not seem to have influenced the air barrier of CNF-C and CNF-T coatings to a large extent. The improvement in air permeability with CNF coating is also well-supported by the print penetration test results in Fig. 9 (b and c). The stain length was doubled with the CNF coating application, indicating a closed surface structure for the coating. However, there were also some dark spots visible on the stains, suggesting the presence of some coating defects or pin holes that may lead to poor barrier performance (Ottesen *et al.* 2017). The base substrate roughness could be another reason for the poor barrier performance, as the low coat weights might end up filling the surface roughness, resulting in a non-uniform surface film.

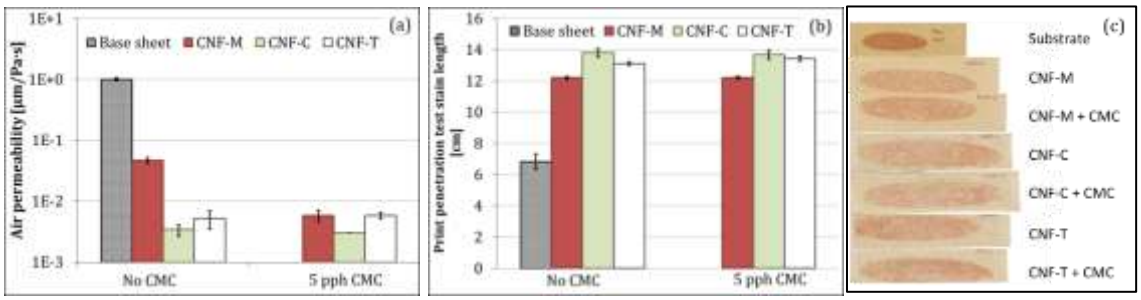

Fig. 9. (a) Air permeability (Ottesen *et al.* 2017) and (b and c) print penetration test stain lengths. Error bars denote standard deviation.

The barrier function of CNF-coated paperboards against water vapor and heptane vapor was also determined. Figure 10 shows the WVTR and HVTR results for the various CNF-coated paperboards. CNF coatings obviously formed a more closed network compared with the substrate, thus leading to a reduction in the WVTR (Fig. 10a). However, this reduction is not sufficient for moisture barrier applications.

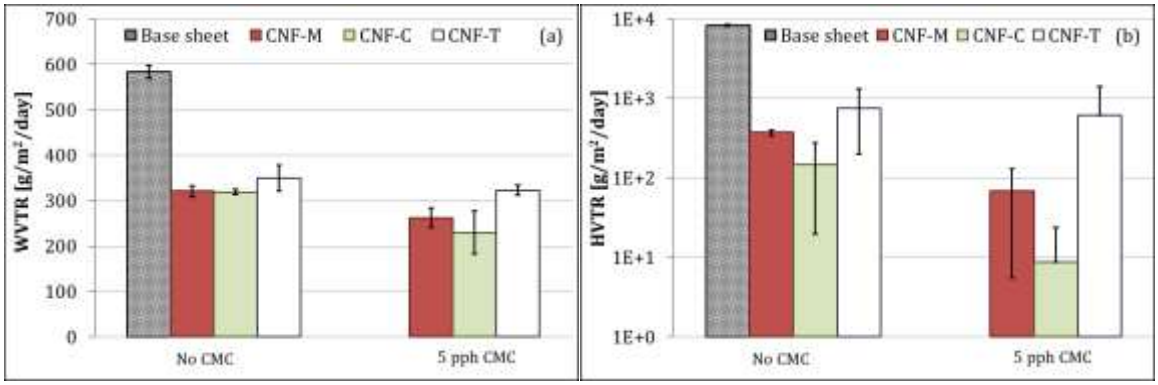

Fig. 10. (a) Water vapor and (b) heptane vapor barrier of CNF coatings. Error bars denote standard deviation.

The food packaging industry constantly faces concerns related to the migration of mineral oil from packaging material to food. This mineral oil can come from printing inks along with recycled fibers utilized in packaging boards. Heptane is one of the components in various mineral oils used in printing inks; therefore, the HVTR can be used as an indicator of the mineral oil barrier performance (Miettinen *et al.* 2015). The HVTR values for CNF-coated paperboards are shown in Fig. 10b. CNF coatings reduce the HVTR substantially, with CNF-C showing the highest reduction. However, the reduction is lower compared with earlier reports (Kumar *et al.* 2016a). The HVTR results also indicate the presence of defects in the CNF coatings.

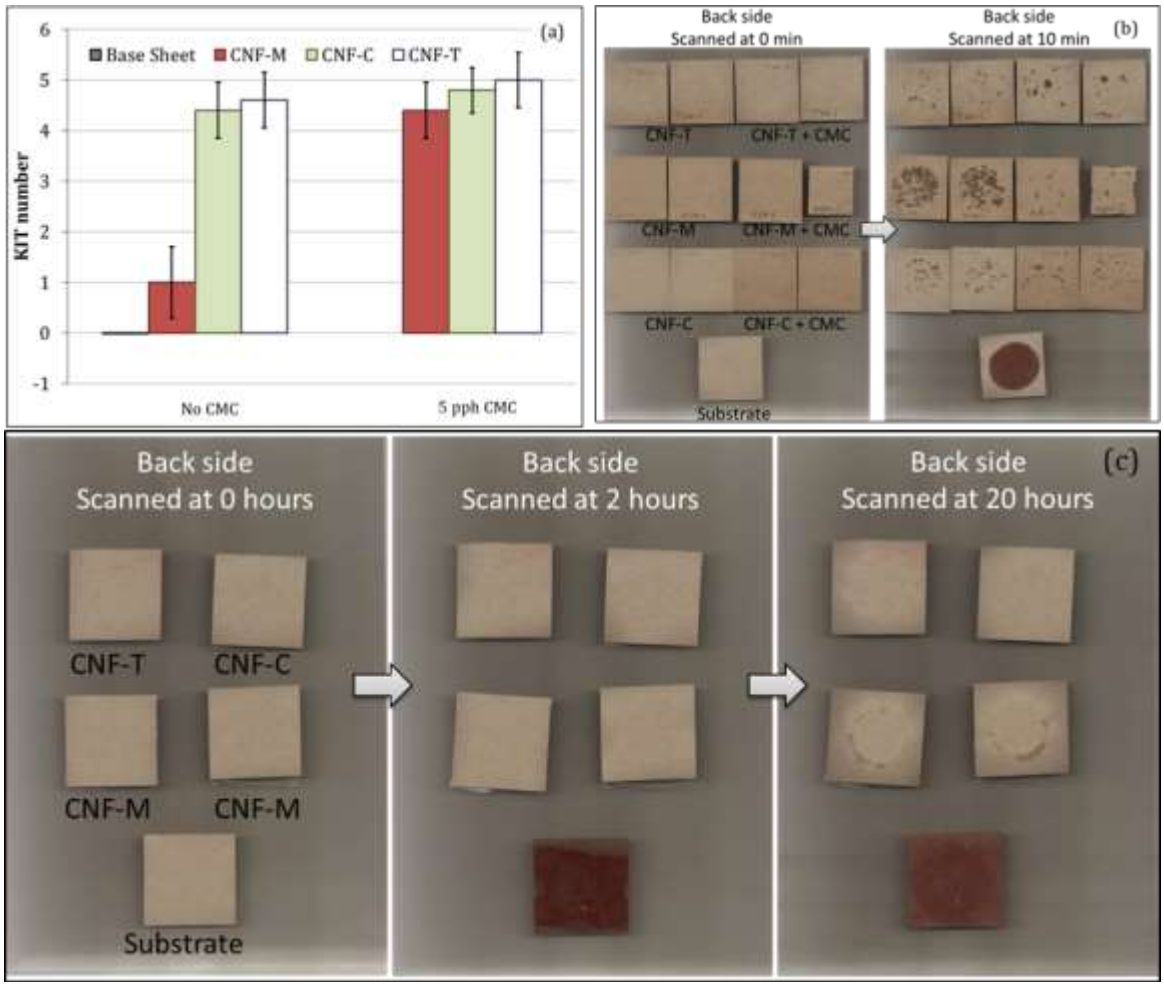

Fig. 11. Results from (a) KIT tests and (b) Oil Red O tests for CNF coatings. (c) Oil Red O tests for 30-µm-thick free-standing CNF films. Error bars denote standard deviation.

A grease barrier is important for several food packaging applications. Grease resistance is usually characterized in the paper and board industry using the KIT test method. Figure 11a shows the KIT test results for CNF-coated paperboards. The KIT number was improved to some extent by CNF-T and CNF-C coatings. The pure CNF-M coating did not seem to have any grease resistance, potentially because of the presence of pin holes or a non-uniform coating. However, the addition of CMC to CNF-M improved the KIT number, indicating a more uniform and/or denser coating structure. CMC addition did not influence the KIT values for CNF-C and CNF-T coatings. Oil Red O test results,

shown in Fig. 11b, also support the KIT results. Overall, the CNF coatings did not seem to provide an optimal grease barrier, as was provided by 30-µm-thick free-standing films of the same materials (Fig. 11c). This indicates that the coating should be improved in terms of thickness either by applying multiple layers or applying single layers at higher CNF concentrations. Defect-free coating is required to achieve optimal barrier performance.

In terms of barrier performance, the low coat weight CNF coatings reported here significantly improve the barrier against air, heptane vapor, and grease; indicating a closed sheet structure obtained with the CNF coating. However, they did not perform well against moisture. This is because the water vapor transport happens through a combination of adsorption and diffusion, and the cellulosic materials are naturally sensitive to moisture and can adsorb and diffuse moisture easily.

CONCLUSIONS

1. The water retention of mechanically produced CNF (CNF-M) was the poorest of all, likely because of the lower charge content and larger fibril diameter compared with carboxymethylated CNF (CNF-C) and TEMPO-oxidized CNF (CNF-T). Although it did not affect the coatability of CNF-M as such, the final coating quality obtained was slightly inferior compared with the other CNFs. High-shear rate rheology (1000 to 20000 s^{-1}) of CNF suspensions determined with the slot-die agreed well with the low-shear rate rheology (0.01 to 1000 s^{-1}) determined with MCR. All CNF suspensions showed shear thinning behavior; this behavior for CNF-T and CNF-C continues as higher shear rates are applied, but for CNF-M, the viscosity seems to reach a Newtonian plateau at approximately 10,000 s^{-1}.
2. CMC addition improved the water retaining capability of CNF suspensions, albeit to varying extents. The water retention of CNF-M was the most affected by CMC addition, but there was no visible influence on the coatability of CNF-M. However, the final coating quality obtained for CNF-M was improved with CMC addition. The coatabilities of CNF-T and CNF-C seemed to improve greatly with CMC addition, but the final coating quality obtained was surprisingly similar to or only slightly improved from the case without CMC addition. CMC addition influenced the rheology of CNF-T and CNF-C to a greater extent than that of CNF-M, as it seems to break down the gel structure of CNF-T and CNF-C. A reduced process viscosity for CNF-T and CNF-C certainly improves their coatability by easier pumping to the slot-die and improved film formation.
3. The chemically pre-treated CNFs were found to provide slightly superior coating in terms of barrier function as compared with CNF-M, likely because of their smaller fibril diameter and narrower fibril size distribution. However, the coat weights applied herein were not found to be sufficient to obtain an optimal barrier for day-to-day packaging applications, likely because of the presence of pin holes and cracks in the coating caused by high brittleness. Insufficient coating coverage caused by the high surface roughness of the base substrate could be another potential reason for the poor barrier performance.
4. The results from these studies indicate that the use of CNFs to create barrier performance is an onerous task, compared with the existing approaches, *e.g.* use of

plastics and pigment coating. In addition to drying, the cost of CNF material is a significant challenge. Future work will explore the coating possibility at higher CNF concentrations and addition of plasticizers to prevent cracks to ensure an optimal barrier.

ACKNOWLEDGEMENTS

This work was performed as a part of the NORCEL Project: The NORwegian NanoCELlulose Technology Platform, initiated and led by The Paper and Fiber Research Institute (PFI) in Trondheim and funded by the Research Council of Norway through the NANO2021 Program (grant 228147 Research Council of Norway). Thanks are extended to Södra, who provided kraft pulp, and to Borregaard for providing bleached sulfite pulp. CNF-T was prepared in collaboration with Silje Neland Molnes. Thanks are also extended to Jonathan Økland Torstensen for supplying us with the CNF-C used in the current work and for discussions concerning the results described and discussed in the current paper. Special thanks to Rajesh Koppolu and Aayush Kumar Jaiswal for assistance during coating of the base board and for discussions during said work.

REFERENCES CITED

Afra, E., Mohammadnejad, S., Saraeyan, A. (2016). "Cellulose nanofibils as coating material and its effects on paper properties," *Prog. Organic Coatings* 101, 455-460. DOI: 10.1016/j.porgcoat.2016.09.018

Agoda-Tandjawa, G., Durand, S., Berot, S., Blassel, C., Gaillard, C., Garnier, C., and Doublier, J. (2010). "Rheological characterization of microfibrillated cellulose suspensions after freezing," *Carbohydr. Polym.* 80(3), 677-686. DOI: 10.1016/j.carbpol.2009.11.045

Ahola, S., Myllytie, P., Österberg, M., Teerinen, T., and Laine, J. (2008). "Effect of polymer adsorption on cellulose nanofibril water binding capacity and aggregation," *BioResources* 3(4), 1315-1328. DOI: 10.15376/biores.3.4.1315-1328

Amini, E., Azadfallah, M., Layeghi, M., and Talaei-Hassanloui, R. (2016). "Silver-nanoparticle-impregnated cellulose nanofiber coating for packaging paper," *Cellulose* 23(1), 1-14. DOI: 10.1007/s10570-015-0846-1

ASTM E96/E96M-05 (2005). "Standard test methods for water vapor transmission of materials," ASTM International, West Conshohocken, PA. DOI: 10.1520/E0096_E0096M-05

Aulin, C., Gällstedt, M., and Lindström, T. (2010). "Oxygen and oil barrier properties of microfibrillated cellulose films and coatings," *Cellulose* 17(3), 559-574. DOI: 10.1007/s10570-009-9393-y

Azeredo, H. M. C., Rosa, M. F., and Mattoso, L. H. C. (2016). "Nanocellulose in bio-based food packaging applications," *Industrial Crops and Products* 97, 664-671. DOI: 10.1016/j.indcrop.2016.03.013

Beghello, L. (1998). "Some factors that influence fiber flocculation," *Nordic Pulp & Paper Research Journal* 13(4), 274-279. DOI: 10.3183/NPPRJ-1998-13-04-p274-279

Beneventi, D., Chaussy, D., Curtil, D., Zolin, L., Gerbaldi, C., and Penazzi, N. (2014). "Highly porous paper loading with microfibrillated cellulose by spray coating on wet substrates," *Ind. Eng. Chem. Res.* 53(27), 10982-10989. DOI: 10.1021/ie500955x

Brodin, F. W., Gregersen, O. W., and Syverud, K. (2014). "Cellulose nanofibrils: Challenges and possibilities as a paper additive or coating material–A review," *Nord. Pulp Pap Res. J.* 29(1), 156-166. DOI: 10.3183/NPPRJ-2014-29-01-p156-166

Cheng, Q., Wang, J., McNeel, J., and Jacobson, P. (2010). "Water retention value measurements of cellulosic materials using a centrifuge technique," *BioResources* 5(3), 1945-1954. DOI: 10.15376/biores.5.3.1945-1954

Dimic-Misic, K. (2014). *Micro and Nanofibrillated Cellulose (MNFC) as Additive in Complex Suspensions: Influence on Rheology and Dewatering,* PhD thesis, Aalto University, Helsinki, Finland.

Eichhorn, S. J., Dufresne, A., Aranguren, M., Marcovich, N. E., Capadona, J. R., Rowan, S. J., Weder, C., Thielemans, W., Roman, M., Renneckar, S., *et al*. (2010). "Review: Current international research into cellulose nanofibres and nanocomposites," *J. Mater. Sci.* 45(1), 1-33. DOI: 10.1007/s10853-009-3874-0

George, J., and Sabapathi, S. (2015). "Cellulose nanocrystals: Synthesis, functional properties, and applications," *Nanotechnology, Science and Applications* 8, 45-54. DOI: 10.2147/NSA.S64386

Haavisto, S., Salmela, J., Jäsberg, A., Saarinen, T., Karppinen, A., and Koponen, A. (2015). "Rheological characterization of microfibrillated cellulose suspension using optical coherence tomography," *TAPPI Journal* 14(5), 291-302.

Habibi, Y., Lucia, L. A., and Rojas, O. J. (2010). "Cellulose nanocrystals: Chemistry, self-assembly, and applications," *Chem. Rev.* 110(6), 3479-3500. DOI: 10.1021/cr900339w

Hamada, H., and Mitsuhashi, M. (2016). "Effect of cellulose nanofibers as a coating agent for woven and nonwoven fabrics," *Nordic Pulp & Paper Research Journal* 31(2), 255-260. DOI: 10.3183/NPPRJ-2016-31-02-p255-260

Herrera, M. A., Sirviö, J. A., Mathew, A. P., and Oksman, K. (2016). "Environmental friendly and sustainable gas barrier on porous materials: Nanocellulose coatings prepared using spin-and dip-coating," *Mater Des* 93, 19-25. DOI: 10.1016/j.matdes.2015.12.127

Herrera, M. A., Mathew, A. P., and Oksman, K. (2017). "Barrier and mechanical properties of plasticized and cross-linked nanocellulose coatings for paper packaging applications," *Cellulose* 24(9), 3969-3980. DOI: 10.1007/s10570-017-1405-8

Hoeng, F., Denneulin, A., and Bras, J. (2016). "Use of nanocellulose in printed electronics: A review," *Nanoscale* 8, 13131-13154. DOI: 10.1039/C6NR03054H

Hua, K. (2015). *Nanocellulose for Biomedical Applications,* PhD thesis, Uppsala University, Uppsala, Sweden.

Hubbe, M., Ferrer, A., Tyagi, P., Yin, Y., Salas, C., Pal, L., and Rojas, O. (2017). "Nanocellulose in thin films, coatings, and plies for packaging applications: A review," *BioResources* 12(1), 2143-2233. DOI: 10.15376/biores.12.1.2143-2233

IGT-W24 (2006). "Print penetration (oil absorption)," IGT Testing Systems, Amsterdam, The Netherlands.

Iotti, M., Gregersen, Ø, Moe, S., and Lenes, M. (2011). "Rheological studies of microfibrillar cellulose water dispersions," *Journal of Polymers and the Environment* 19(1), 137-145. DOI: 10.1007/s10924-010-0248-2

Isogai, A., Saito, T., and Fukuzumi, H. (2011). "TEMPO-oxidized cellulose nanofibers," *Nanoscale* 3(1), 71-85. DOI: 10.1039/c0nr00583e

Isogai, A. (2013). "Wood nanocelluloses: Fundamentals and applications as new bio-based nanomaterials," *Journal of Wood Science* 59(6), 449-459. DOI: 10.1007/s10086-013-1365-z

Johansson, C., Bras, J., Mondragon, I., Nechita, P., Plackett, D., Simon, P., Svetec, D. G., Virtanen, S., Baschetti, M. G., and Breen, C. (2012). "Renewable fibers and bio-based materials for packaging applications: a review of recent developments," *BioResources* 7(2), 2506-2552. DOI: 10.15376/biores.7.2.2506-2552

Jorfi, M., and Foster, E. J. (2015). "Recent advances in nanocellulose for biomedical applications," *J. Appl. Polym. Sci.* 132(14), 41719. DOI: 10.1002/app.41719

Khalil, H. P. S. A., Saurabh, C. K., A.S., A., Nurul Fazita, M. R., Syakir, M. I., Davoudpour, Y., Rafatullah, M., Abdullah, C. K., M. Haafiz, M. K., and Dungani, R. (2016). "A review on chitosan-cellulose blends and nanocellulose reinforced chitosan biocomposites: Properties and their applications," *Carbohydr. Polym.* 150, 216-226. DOI: 10.1016/j.carbpol.2016.05.028

Khan, A., Huq, T., Khan, R. A., Riedl, B., and Lacroix, M. (2014). "Nanocellulose-based composites and bioactive agents for food packaging," *Crit. Rev. Food Sci. Nutr.* 54(2), 163-174. DOI: 10.1080/10408398.2011.578765

Kim, J., Shim, B. S., Kim, H. S., Lee, Y., Min, S., Jang, D., Abas, Z., and Kim, J. (2015). "Review of nanocellulose for sustainable future materials," *International Journal of Precision Engineering and Manufacturing-Green Technology* 2(2), 197-213. DOI: 10.1007/s40684-015-0024-9

Kinnunen-Raudaskoski, K., Hjelt, T., Kenttä, E., and Forsström, U. (2014). "Thin coatings for paper by foam coating," *TAPPI Journal* 13(7), 9-19.

Klemm, D., Kramer, F., Moritz, S., Lindström, T., Ankerfors, M., Gray, D., and Dorris, A. (2011). "Nanocelluloses: A new family of nature-based materials," *Angewandte Chemie International Edition* 50(24), 5438-5466. DOI: 10.1002/anie.201001273

Kumar, V., Bollström, R., Yang, A., Chen, Q., Chen, G., Salminen, P., Bousfield, D., and Toivakka, M. (2014). "Comparison of nano-and microfibrillated cellulose films," *Cellulose* 21(5), 3443-3456. DOI: 10.1007/s10570-014-0357-5

Kumar, V., Elfving, A., Koivula, H., Bousfield, D., and Toivakka, M. (2016a). "Roll-to-roll processed cellulose nanofiber coatings," *Ind Eng Chem Res* 55(12), 3603-3613. DOI: 10.1021/acs.iecr.6b00417

Kumar, V., Nazari, B., Bousfield, D. W., and Toivakka, M. (2016b). "Rheology of microfibrillated cellulose suspensions in pressure-driven flow," *Applied Rheology* 26(4), 43534. DOI: 10.3933/APPLRHEOL-26-43534

Kumar, V., Koppolu, V. R., Bousfield, D., and Toivakka, M. (2017). "Substrate role in coating of microfibrillated cellulose suspensions," *Cellulose* 24(3), 1247-1260. DOI: 10.1007/s10570-017-1201-5

Lahtinen, P., Liukkonen, S., Pere, J., Sneck, A., and Kangas, H. (2014). "A comparative study of fibrillated fibers from different mechanical and chemical pulps," *BioResources* 9(2), 2115-2127. DOI: 10.15376/biores.9.2.2115-2127

Lasseuguette, E., Roux, D., and Nishiyama, Y. (2008). "Rheological properties of microfibrillar suspension of TEMPO-oxidized pulp," *Cellulose* 15(3), 425-433. DOI: 10.1007/s10570-007-9184-2

Lavoine, N., Bras, J., and Desloges, I. (2014a). "Mechanical and barrier properties of cardboard and 3D packaging coated with microfibrillated cellulose," *J. Appl. Polym. Sci.* 131(8), 40106. DOI: 10.1002/app.40106

Lavoine, N., Desloges, I., Khelifi, B., and Bras, J. (2014b). "Impact of different coating processes of microfibrillated cellulose on the mechanical and barrier properties of paper," *J. Mater. Sci.* 49(7), 2879-2893. DOI: 10.1007/s10853-013-7995-0

Lavoine, N., Desloges, I., Dufresne, A., and Bras, J. (2012). "Microfibrillated cellulose – Its barrier properties and applications in cellulosic materials: A review," *Carbohydr. Polym.* 90(2), 735-764. DOI: 10.1016/j.carbpol.2012.05.026

Lee, K., Aitomäki, Y., Berglund, L. A., Oksman, K., and Bismarck, A. (2014). "On the use of nanocellulose as reinforcement in polymer matrix composites," *Composites Sci. Technol.* 105, 15-27. DOI: 10.1016/j.compscitech.2014.08.032

Li, F., Mascheroni, E., and Piergiovanni, L. (2015). "The potential of nanocellulose in the packaging field: A review," *Packaging Technology and Science* 28(6), 475-508. DOI: 10.1002/pts.2121

Liimatainen, H., Haavisto, S., Haapala, A., and Niinimäki, J. (2009). "Influence of adsorbed and dissolved carboxymethyl cellulose on fibre suspension dispersing, dewaterability, and fines retention," *BioResources* 4(1), 321-340. DOI: 10.15376/biores.4.1.321-340

Lin, N., and Dufresne, A. (2014). "Nanocellulose in biomedicine: Current status and future prospect," *European Polymer Journal* 59, 302-325. DOI: 10.1016/j.eurpolymj.2014.07.025

Liu, J., Chinga-Carrasco, G., Cheng, F., Xu, W., Willför, S., Syverud, K., and Xu, C. (2016). "Hemicellulose-reinforced nanocellulose hydrogels for wound healing application," *Cellulose* 23(5), 3129-3143. DOI: 10.1007/s10570-016-1038-3

Marchessault, R. H., Morehead, F. F., and Walter, N. M. (1959). "Liquid crystal systems from fibrillar polysaccharides," *Nature* 184(4686), 632-633. DOI: 10.1038/184632a0

Mariano, M., El Kissi, N., and Dufresne, A. (2014). "Cellulose nanocrystals and related nanocomposites: review of some properties and challenges," *Journal of Polymer Science Part B: Polymer Physics* 52(12), 791-806. DOI: 10.1002/polb.23490

Miettinen, P., Kuusipalo, J., Auvinen, S., Haakana, S. (2015). "Validity of traditional barrier-testing methods to predict the achievable benefits of the new generation water based barrier coatings for packaging materials," *in: 27th PTS Coating Symposium*, September 16-18, Munich, Germany, pp. 328-342.

Moberg, T., Rigdahl, M., Stading, M., and Levenstam Bragd, E. (2014). "Extensional viscosity of microfibrillated cellulose suspensions," *Carbohydr. Polym.* 102(0), 409-412. DOI: 10.1016/j.carbpol.2013.11.041

Mohtaschemi, M., Dimic-Misic, K., Puisto, A., Korhonen, M., Maloney, T., Paltakari, J., and Alava, M. J. (2014). "Rheological characterization of fibrillated cellulose suspensions via bucket vane viscometer," *Cellulose* 21(3), 1305-1312. DOI: 10.1007/s10570-014-0235-1

Moon, R. J., Martini, A., Nairn, J., Simonsen, J., and Youngblood, J. (2011). "Cellulose nanomaterials review: Structure, properties and nanocomposites," *Chem. Soc. Rev.* 40(7), 3941-3994. DOI: 10.1039/C0CS00108B

Mousavi, S. M., Afra, E., Tajvidi, M., Bousfield, D., and Dehghani-Firouzabadi, M. (2017). "Cellulose nanofiber/carboxymethyl cellulose blends as an efficient coating to improve the structure and barrier properties of paperboard," *Cellulose* 24(7), 3001-3014. DOI: 10.1007/s10570-017-1299-5

Naderi, A., and Lindström, T. (2014). "Carboxymethylated nanofibrillated cellulose: Effect of monovalent electrolytes on the rheological properties," *Cellulose* 21(5), 3507-3514. DOI: 10.1007/s10570-014-0394-0

Naderi, A., and Lindström, T. (2015). "Rheological measurements on nanofibrillated cellulose systems: A science in progress," in: *Cellulose and Cellulose Derivatives: Synthesis, Modification and Applications*, M. I. H. Mondal (eds.), Nova Science, New York, USA, pp. 187-202.

Naderi, A., and Lindström, T. (2016). "A comparative study of the rheological properties of three different nanofibrillated cellulose systems," *Nordic Pulp & Paper Research Journal* 31(3), 354-363. DOI: 10.3183/NPPRJ-2016-31-03-p354-363

Nazari, B., Kumar, V., Bousfield, D. W., and Toivakka, M. (2016). "Rheology of cellulose nanofibers suspensions: Boundary driven flow," *J. Rheol.* 60(6), 1151-1159. DOI: 10.1122/1.4960336

Nechyporchuk, O., Belgacem, M. N., and Pignon, F. (2014). "Rheological properties of micro-/nanofibrillated cellulose suspensions: Wall-slip and shear banding phenomena," *Carbohydr. Polym.* 112, 432-439. DOI: 10.1016/j.carbpol.2014.05.092

Nechyporchuk, O., Belgacem, M. N., and Bras, J. (2016a). "Production of cellulose nanofibrils: A review of recent advances," *Industrial Crops and Products* 93, 2-25. DOI: 10.1016/j.indcrop.2016.02.016

Nechyporchuk, O., Belgacem, M. N., and Pignon, F. (2016b). "Current progress in rheology of cellulose nanofibril suspensions," *Biomacromolecules* 17(7), 2311-2320. DOI: 10.1021/acs.biomac.6b00668

Nickerson, R. F., and Habrle, J. A. (1947). "Cellulose intercrystalline structure," *Industrial and Engineering Chemistry* 39(11), 1507-1512. DOI: 10.1021/ie50455a024

Nikbakht, A., Madani, A., Olson, J. A., and Martinez, D. M. (2014). "Fibre suspensions in Hagen–Poiseuille flow: Transition from laminar plug flow to turbulence," *J. Non Newtonian Fluid Mech.* 212(0), 28-35. DOI: 10.1016/j.jnnfm.2014.08.006

Osong, S. H., Norgren, S., and Engstrand, P. (2016). "Processing of wood-based microfibrillated cellulose and nanofibrillated cellulose, and applications relating to papermaking: A review," *Cellulose* 23(1), 93-123. DOI: 10.1007/s10570-015-0798-5

Ottesen, V., Kumar, V., Toivakka, M., Chinga-Carrasco, G., Syverud, K., and Gregersen, Ø W. (2017). "Viability and properties of roll-to-roll coating of cellulose nanofibrils on recycled paperboard," *Nordic Pulp & Paper Research Journal* 32(2), 179-188. DOI: 10.3183/NPPRJ-2017-32-02-p179-188

Pääkkö, M., Ankerfors, M., Kosonen, H., Nykänen, A., Ahola, S., Österberg, M., Ruokolainen, J., Laine, J., Larsson, P. T., Ikkala, O., *et al*. (2007). "Enzymatic hydrolysis combined with mechanical shearing and high-pressure homogenization for nanoscale cellulose fibrils and strong gels," *Biomacromolecules* 8(6), 1934-1941. DOI: 10.1021/bm061215p

Paunonen, S. (2013). "Nanocellulose-based food packaging materials - A Review," *Nordic Pulp & Paper Research Journal* 28(2), 165-181. DOI: 10.3183/NPPRJ-2013-28-02-p165-181

Plackett, D. V., Letchford, K., Jackson, J. K., and Burt, H. M. (2014). "A review of nanocellulose as a novel vehicle for drug delivery," *Nordic Pulp & Paper Research Journal* 29(1), 105-118. DOI: 10.3183/NPPRJ-2014-29-01-p105-118

Ramires, E. C., and Dufresne, A. (2011). "A review of cellulose nanocrystals and nanocomposites," *TAPPI Journal* 10(4), 9-16.

Rånby, B. G. (1949). "Aqueous colloidal solutions of cellulose micelles," *Acta Chemica Scandinavica* 3, 649-650. DOI: 10.3891/acta.chem.scand.03-0649

Rantanen, J., Dimic-Misic, K., Pirttiniemi, J., Kuosmanen, P., and Maloney, T. (2015). "Forming and dewatering of a microfibrillated cellulose composite paper," *BioResources* 10(2), 3492-3506. DOI: 10.15376/biores.10.2.3492-3506

Ridgway, C. J., and Gane, P. A. (2012). "Constructing NFC-pigment composite surface treatment for enhanced paper stiffness and surface properties," *Cellulose* 19(2), 547-560. DOI: 10.1007/s10570-011-9634-8

Saito, T., Nishiyama, Y., Putaux, J., Vignon, M., and Isogai, A. (2006). "Homogeneous suspensions of individualized microfibrils from TEMPO-catalyzed oxidation of native cellulose," *Biomacromolecules* 7(6), 1687-1691. DOI: 10.1021/bm060154s

Saito, T., Kimura, S., Nishiyama, Y., and Isogai, A. (2007). "Cellulose nanofibers prepared by TEMPO-mediated oxidation of native cellulose," *Biomacromolecules* 8(8), 2485-2491. DOI: 10.1021/bm0703970

Saito, T., and Isogai, A. (2004). "TEMPO-mediated oxidation of native cellulose. The effect of oxidation conditions on chemical and crystal structures of the water-insoluble fractions," *Biomacromolecules* 5(5), 1983-1989. DOI: 10.1021/bm0497769

Salas, C., Nypelö, T., Rodriguez-Abreu, C., Carrillo, C., and Rojas, O. J. (2014). "Nanocellulose properties and applications in colloids and interfaces," *Current Opinion in Colloid & Interface Science* 19(5), 383-396. DOI: 10.1016/j.cocis.2014.10.003

Sandas, S., Salminen, P. J., and Eklund, D. (1989). "Measuring the water retention of coating colors," *Tappi J.* 72(12), 207-210.

Schenker, M., Schoelkopf, J., Mangin, P., and Gane, P. (2016). "Rheological investigation of complex micro and nanofibrillated cellulose (MNFC) suspensions: Discussion of flow curves and gel stability," *TAPPI Journal* 15(6), 405-416.

Siqueira, G., Bras, J., and Dufresne, A. (2010). "Cellulosic bionanocomposites: A review of preparation, properties and applications," *Polymers* 2(4), 728-765. DOI: 10.3390/polym2040728

Song, H., Anderfors, M., Hoc, M., and Lindström, T. (2010). "Reduction of the linting and dusting propensity of newspaper using starch and microfibrillated cellulose," *Nordic Pulp & Paper Research Journal* 25(4), 495-504. DOI: 10.3183/NPPRJ-2010-25-04-p495-504

Spence, K., Habibi, Y., and Dufresne, A. (2011). "Nanocellulose-based composites," in: *Cellulose Fibers: Bio- and Nano-Polymer Composites: Green Chemistry and Technology*, S. Kalia, S. B. Kaith, and I. Kaur (eds.), Springer, Berlin, Germany, pp. 179-213.

Syverud, K., and Stenius, P. (2009). "Strength and barrier properties of MFC films," *Cellulose* 16(1), 75-85. DOI: 10.1007/s10570-008-9244-2

Syverud, K., Chinga-Carrasco, G., Toledo, J., and Toledo, P. G. (2011). "A comparative study of *Eucalyptus* and *Pinus radiata* pulp fibres as raw materials for production of cellulose nanofibrils," *Carbohydr. Polym.* 84(3), 1033-1038. DOI: 10.1016/j.carbpol.2010.12.066

TAPPI T 559 pm-96 (1996). "Grease resistance test for paper and paperboard," TAPPI Press, Atlanta, GA.

Turbak, A. F., Snyder, F. W., and Sandberg, K. R. (1983). "Microfibrillated cellulose, a new cellulose product: properties, uses, and commercial potential," *J. Appl. Polym. Sci.: Appl. Polym. Symp.* 37, 815-823.

Vähä-Nissi, M. (2016). "Test methods for evaluating grease and mineral oil barriers," *in: TAPPI PLACE Conference*, 11-13 April, Fort Worth, Texas, USA, pp. 949-970.

Vesterinen, A., Myllytie, P., Laine, J., and Seppälä, J. (2010). "The effect of water-soluble polymers on rheology of microfibrillar cellulose suspension and dynamic mechanical properties of paper sheet," *J. Appl. Polym. Sci.* 116(5), 2990-2997. DOI: 10.1002/app.31832

Wågberg, L., Decher, G., Norgren, M., Lindström, T., Ankerfors, M., and Axnäs, K. (2008). "The build-up of polyelectrolyte multilayers of microfibrillated cellulose and cationic polyelectrolytes," *Langmuir* 24(3), 784-795. DOI: 10.1021/la702481v

Yan, H., Lindström, T., and Christiernin, M. (2006). "Some ways to decrease fibre suspension flocculation and improve sheet formation," *Nordic Pulp & Paper Research Journal* 21(1), 36-43. DOI: 10.3183/NPPRJ-2006-21-01-p036-043

Zheng, G., Cui, Y., Karabulut, E., Wågberg, L., Zhu, H., and Hu, L. (2013). "Nanostructured paper for flexible energy and electronic devices," *MRS Bull* 38(04), 320-325. DOI: 10.1557/mrs.2013.59

Article submitted: May 17, 2017; Peer review completed: July 8, 2017; Revised version received and accepted: August 9, 2017; Published: September 1, 2017.
DOI: 10.15376/biores.12.4.7656-7679